Supporting Information for

Modifying Membrane Morphology and Interactions with DNA Origami Clathrin-Mimic Networks

[§]Céline M. A. Journot, [†]Vivek Ramakrishna, [†]Mark I. Wallace and [§]Andrew J. Turberfield

List of Figures

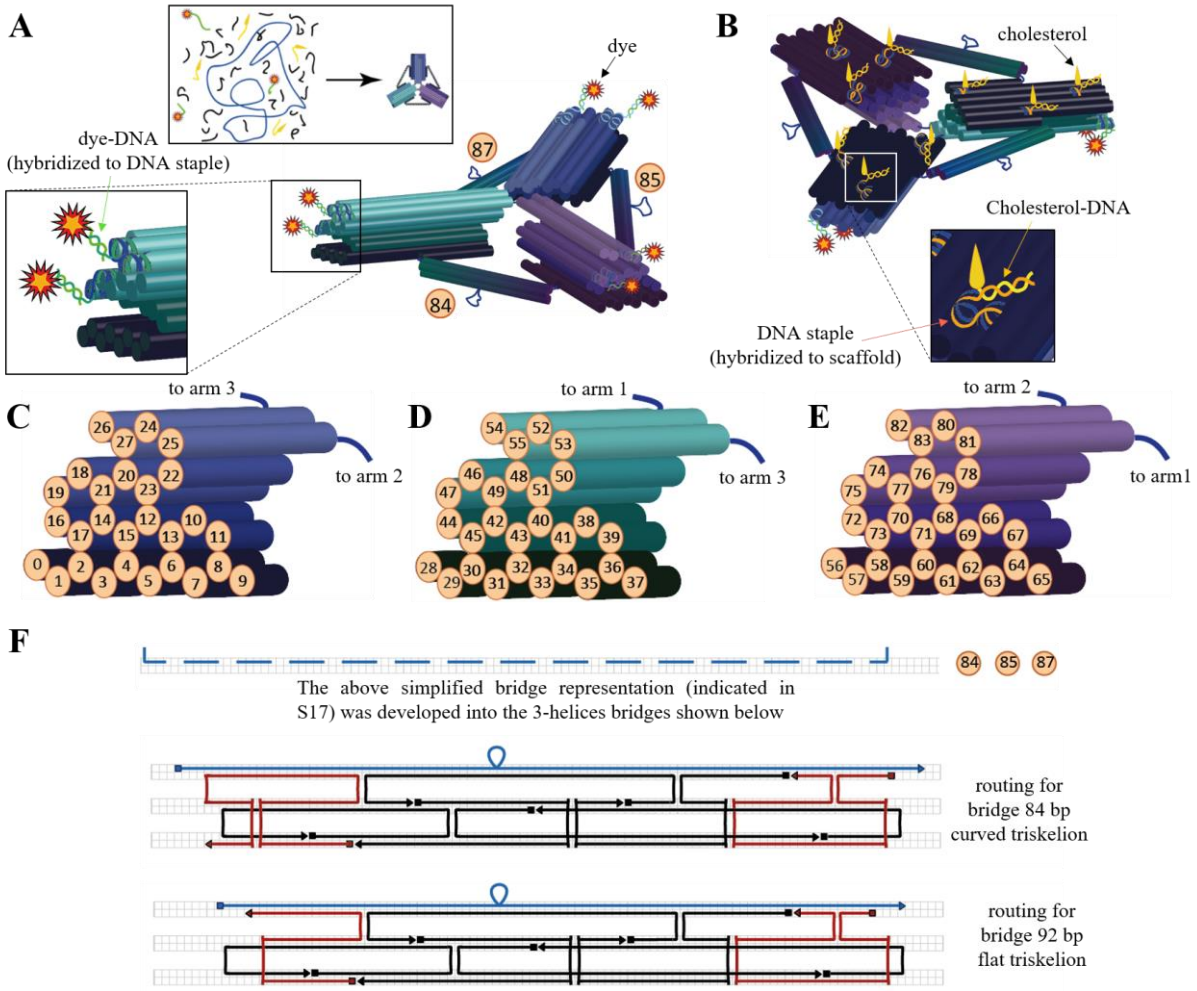

Figure S1: DNA origami triskelion. (A, B) Top (**A**) and bottom (**B**) views showing the three arms and connecting bridges. Each cylinder represents a DNA helix, numbered as in the Cagnino design file (Supplementary Figure $17); these numbers are used to identify the positions of staple strands (cf. 'DNA Sequences') in the assembly. Note that the arms are viewed from their outer extremities; Fig $17 shows the numbering of the helices viewed from the center of the triskelia. DNA staple strands bearing dye and cholesterol moieties are included in the folding mix (in 10 times excess relative to the scaffold concentration) during annealing of the origami (inset). These functionalized strands bind to complementary overhangs of DNA staples which are incorporated in the origami during folding (as detailed in the two enlargement boxes). Excess conjugates are removed with the other DNA staples. Alexa647-DNA conjugates are attached to the upper layers of DNA helices (see enlarged inset of (**A**)) in helices that are not involved in linking (polymerization) of the triskelia. Cholesterol-DNA conjugates are attached to the bottom layer, as detailed in the enlarged inset of (**B**). (**C**-**E**) Cross-section of arm 1 (**C**), arm 2 (**D**) and arm 3 (**E**). Helices 0 and 9 of arm 1, 28 and 37 of arm 2, and 56 and 65 of arm 3 stop at mid-length to become the bridges (helix 84 links arms 2 and 3, 85 links arms 1 and 3, and 87 links arms 1 and 2, also indicated in (**A**)). (**F**) Bridge designs. The blue line represents the DNA scaffold which runs through the whole DNA origami; the rest of the structure is made up of shorter oligonucleotides. Those shown in red have sequences specific to the two lengths of bridge, those in black are common to both lengths. The scaffold loop part way along the bridge provides a reservoir of bases to allow for bridges of different lengths. Loop lengths for flat triskelia: 30 bases (helix 84) and 29 bases (helices 85, 87. Loop lengths for curved triskelia: 38 bases (helix 84); 37 bases (helices 85, 87).

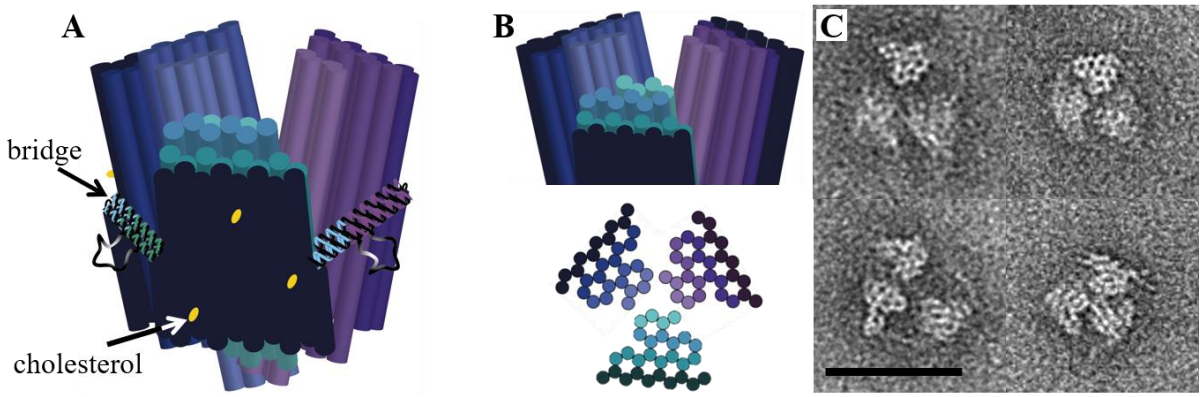

Figure S2: Identification of convex triskelia from TEM micrographs. (**A**) Illustration of the curved triskelion with arms raised out-of-plane, showing the cholesterol anchors on the outside. (**B**) Cross sections of the arms showing the component DNA helices, and (**C**) electron micrographs of curved triskelia monomers showing the same honeycomb lattice as the model. Scale bars 50 nm.

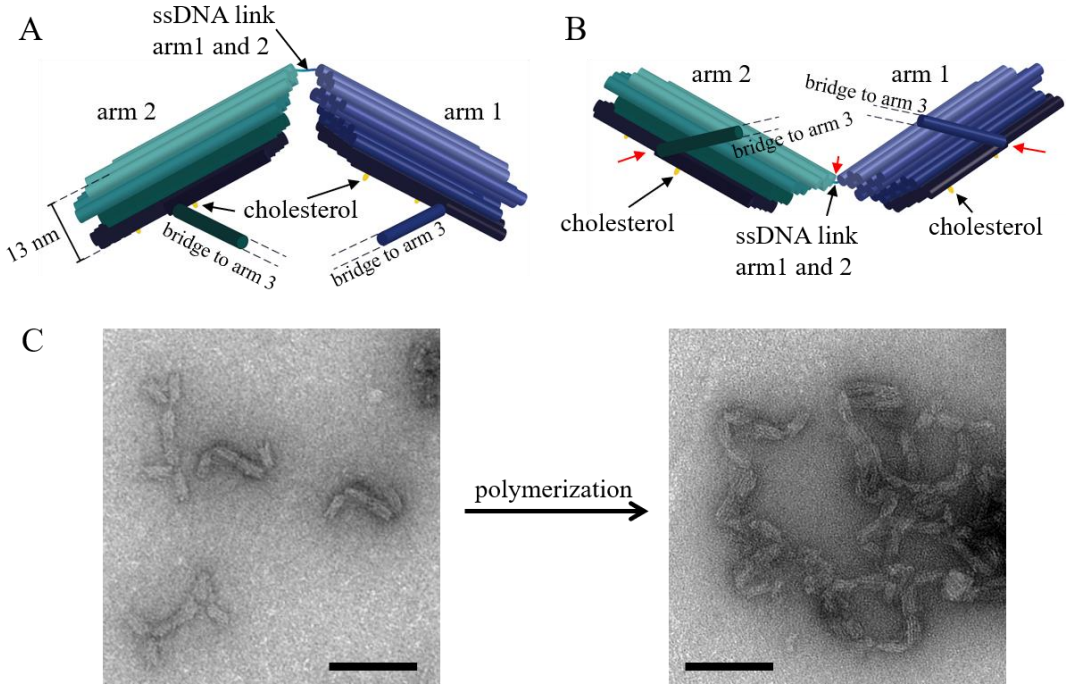

Figure S3: **Two conformations of curved triskelia**. (**A**) Schematic representation of a curved triskelion that is curved such that the cholesterol modifications lie on the concave, inside, surface. Arm 3 is omitted for visibility. The positions of the bridges, and the progressive shortening of the helices at the ends of the arms were intended to favor this configuration. (**B**) Schematic representation of a curved triskelia with cholesterol on the convex, outside, surface. The formation of this conformation was unexpected, and we infer that it is made possible by the disruption of small DNA domains at the ends of the bridges and where the three arms meet (red arrows). (**C**) Electron micrographs showing triskelion dimers, formed by linking arms 1 end-to-end (Supporting Figure S4), in which one triskelion is in the convex configuration and one concave. Also shown is the polymer that results from the addition of links between arms 2 and 3. Scale bars 100 nm.

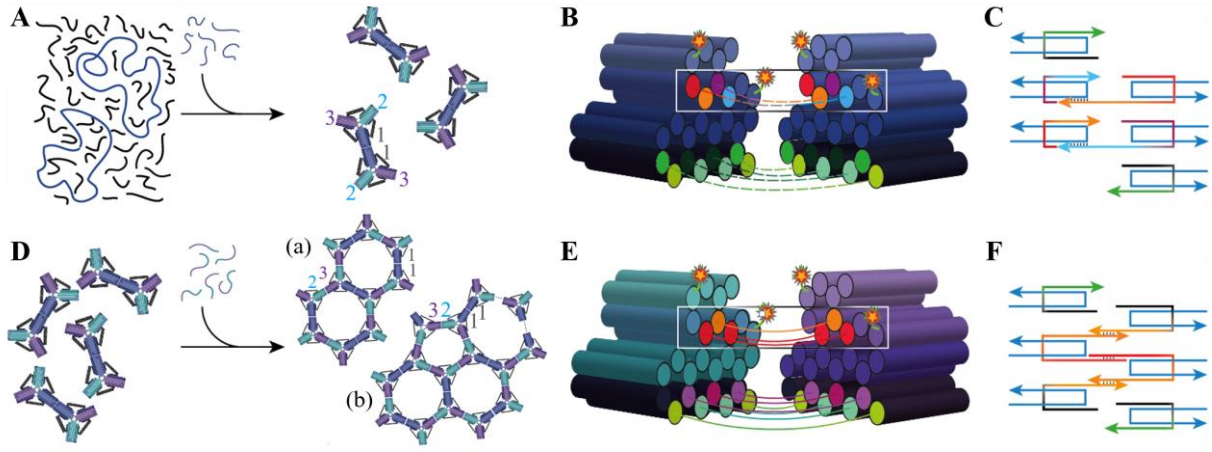

Figure S4: Formation and polymerization of triskelion dimers. (**A**) Schematic of triskelion dimers folding from a mixture of origami staples and scaffold. The staples to connect the two triskelia into a dimer are included in the folding mix and hybridize to scaffold domains in both of the linked Arms 1 (connecting 1↔1). (**B**) 3D representation of the extremities of triskelion Arms 1 illustrating the 6 connections formed by the 6 dimerization staples. Cylinders represent DNA helices. A white box indicates two dimerization staples whose connections are shown in schematic (**C**). Each dimerization staple, when fully inserted, is hybridized at its 5′ end to the scaffold at Arm 1 of one triskelion and at its 3′ end to the scaffold of Arm 1 of a second triskelion. The origami scaffold is shown in dark blue. (**D**) Schematic of polymerization of triskelion dimers triggered by the addition of polymerization staples. Hexagon-only lattices form a flat array (a); the inclusion of pentagonal cells enables curvature (b). (**E**) Polymerization is induced by the addition of polymerization staples which hybridize to the scaffold at the ends of Arms 2 and 3 (separately), displaying single-stranded overhangs (sticky ends). Hybridization of complementary sticky ends links Arms 2 and 3 (2↔3). Connections formed by the polymerization staples indicated by the white box are represented in (**F**).

The sticky ends were designed with the following considerations:

1. the orientation of the sticky ends allows hybridization to form DNA helices that are collinear with the helices of the arms: a 3′ end faces a 5′ end;
2. the sequences of the sticky ends are unique and non-palindromic;
3. no more than two consecutive occurrences of the same base were allowed.

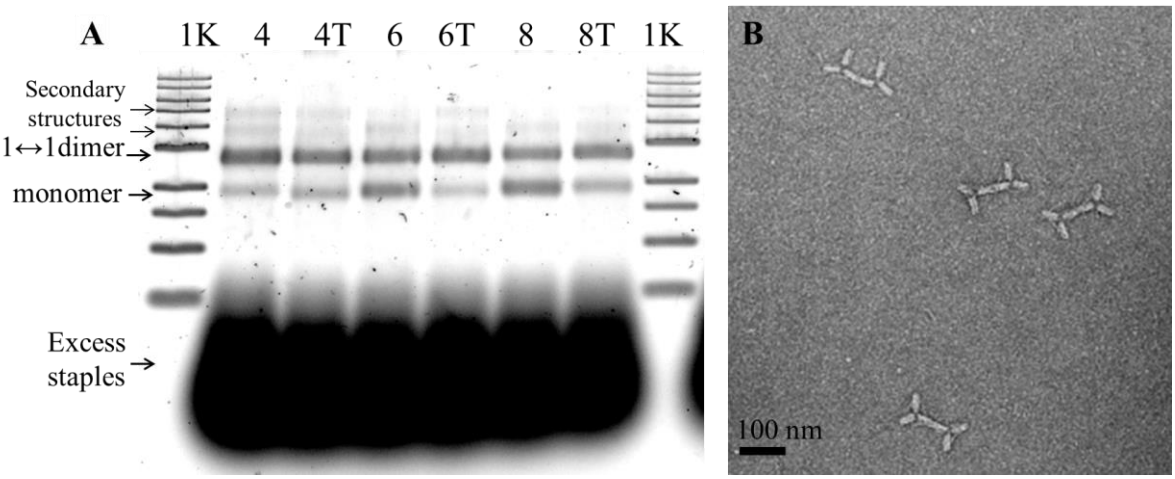

Figure S5: Optimization of the formation of dimers. (**A**) Agarose gel electrophoresis showing the different yields of dimers after origami folding. The number above the wells indicates the number of nucleotides of the shorter of the two domains of each dimerization staple that hybridizes to the scaffold of one of the two component triskelia. A 'T' signifies that, to prevent non-specific helix stacking interactions: a spacer of three Ts is added between the two domains of the dimerization staples; staples that terminate at the interface are extended by $T_{3;}$ and a T_6 loop is added to staple crossovers at the interface. A ladder of 1kbp (1K) is placed for reference on each side of the gel. Analysis of the band intensities was made using ImageJ and gave a maximum yield of 75% dimers for the lane labelled 6T. (**B**) Electron micrographs of triskelion dimers extracted from the gel, lane 6T.

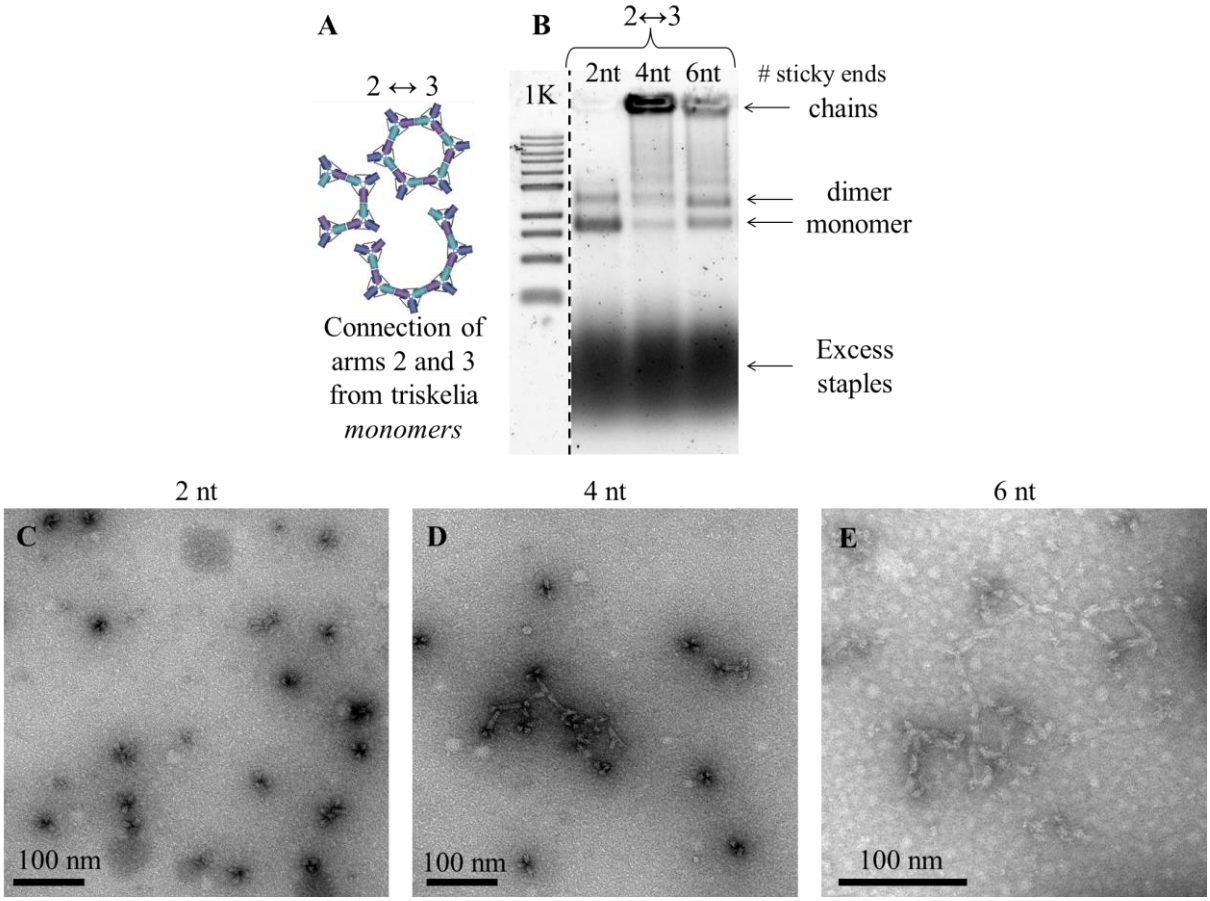

Figure S6: Polymerization staples: sticky end lengths. Triskelion monomers were used during optimization of the length of the sticky ends. The same design parameters were used for dimers, which which share the same arm 2↔3 interface. (**A**) Schematic showing possible products when Arms 2 and 3 of triskelion monomers are connected by polymerization staples: Arms 1 are not connected. (**B**) Agarose gel showing triskelion monomers after addition of polymerization staples with 2-nt, 4-nt and 6-nt sticky ends, sample incubated at 20°C for 2 hours. Slower migration indicates that the triskelia have polymerized. With 2-nt sticky ends there is no signs of polymerization; with both 4- and 6-nt sticky ends, extended polymers accumulate in the well. Sticky ends of 4 nt polymerize faster than 6 nt, indicated by greater accumulation in the well. (**C-E**) TEM micrographs of the same samples after 6 hours at 20°C. Sticky ends of 2 nt remain unpolymerized. At this time point 6-nt sticky ends produced larger chains than 4-nt sticky ends. For this reason, 6-nt sticky ends were selected for subsequent experiments with both triskelion monomers and dimers.

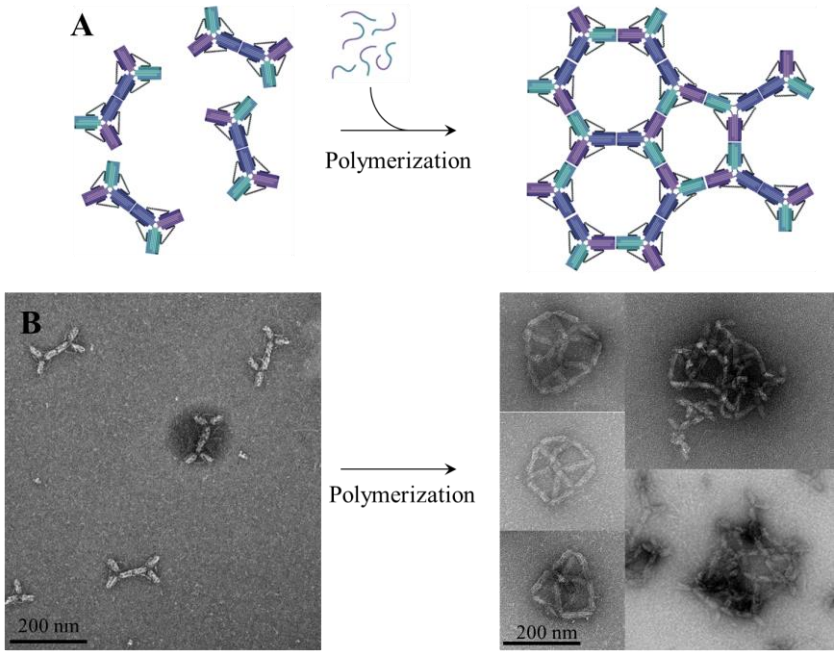

Figure S7: Triskelion networks formed in solution. (**A**) Schematic representation of (left) triskelion dimers and (right) polymerized networks. (**B**) Electron micrographs of triskelion dimers, in the absence of a membrane, (left) before and (right) after addition of 6T polymerization staples. Polymerized dimers form small, closed, polyhedral clusters or disordered aggregates.

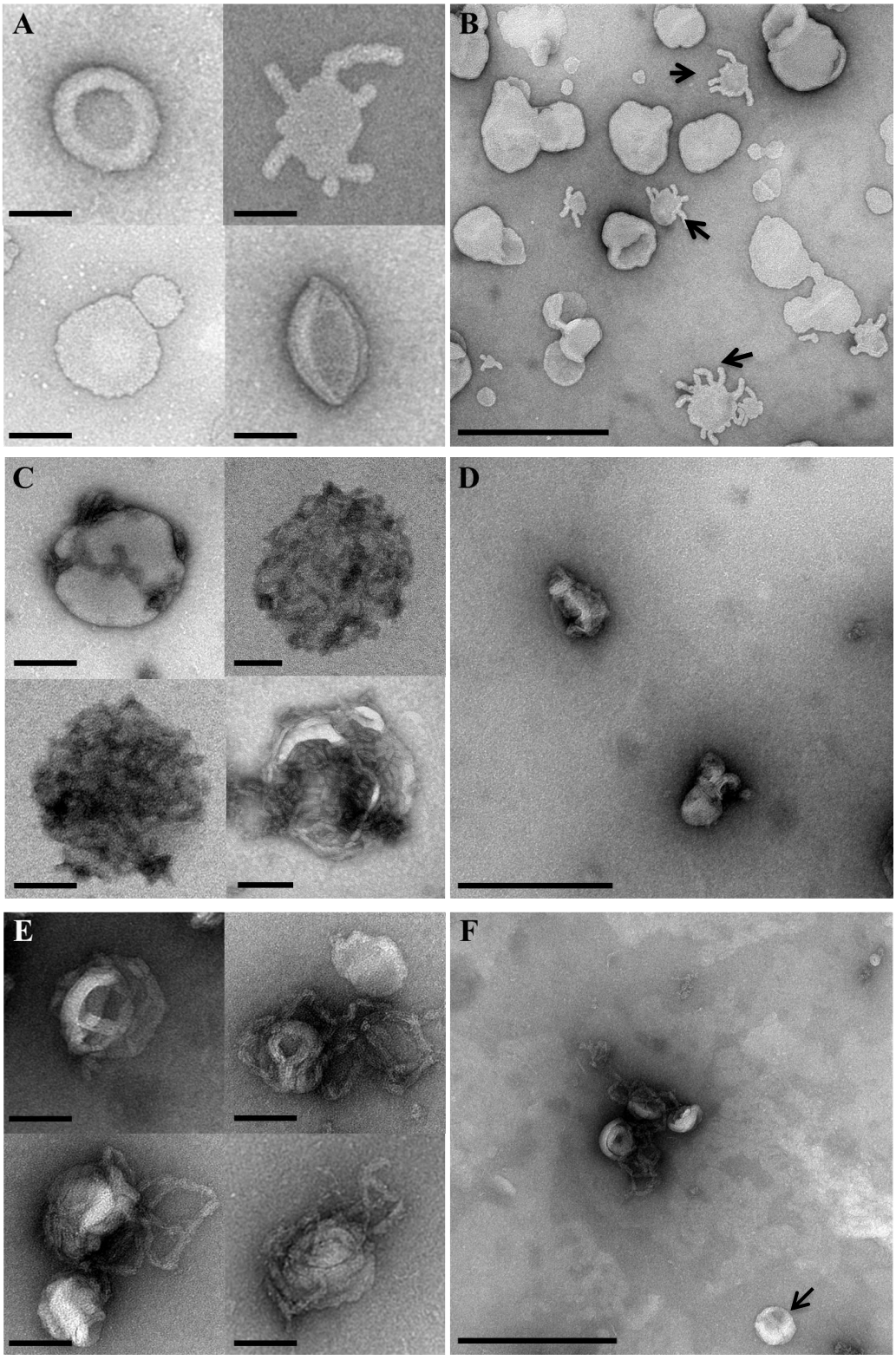

Figure S8: TEM micrographs of polymerized triskelia on SUVs. (**A**, **B**) liposomes without triskelia (control), some of which show tubulations (arrows). (**C**, **D**) Flat triskelia on liposomes. The liposomes, coated with triskelia, are positively stained. (**E**, **F**) curved triskelia on liposomes, stained under the same conditions. A liposome without triskelia in (**F**) is indicated by a black arrow. Scale bars for (**A**), (**C**) and (**E**) 100 nm; scale bars for (**B**), (**D**) and (**F**) 500 nm.

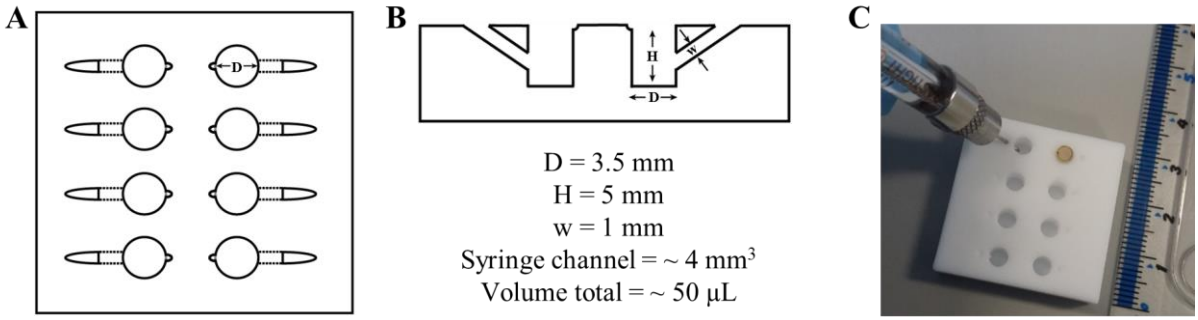

Figure S9: Apparatus used to prepare triskelia interacting with lipid monolayers for electron microscopy. (A, B) Plan, cross-section and dimensions of the Teflon™ block. (C) Photograph of the apparatus with one gold grid on top of a buffer droplet in a well and a syringe inserted in the top left channel for demonstration.

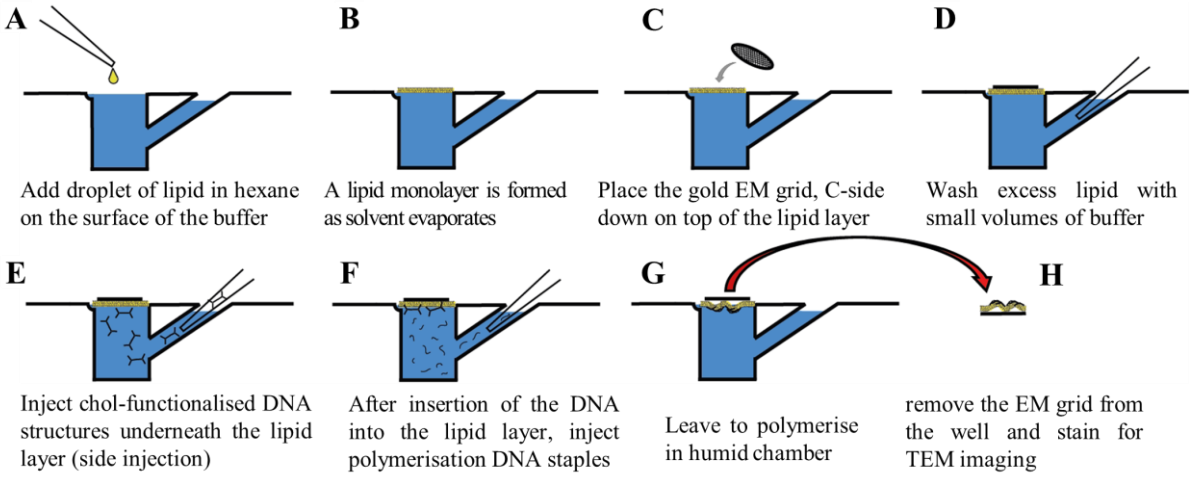

Figure S10: Protocol for the lipid monolayer assay. (**A, B**) A lipid monolayer is first formed at the surface of the buffer and (**C**) an EM grid is placed on top. (**D**) Small volumes of fresh buffer are injected and removed to remove unattached lipid membranes from the well, followed by (**E**) the injection of triskelia dimers under the grid. (**F**) Polymerization staples are then added and (**G**) the wells are left in a humid chamber to allow polymerization. (**H**) The grid is then removed for staining and imaging.

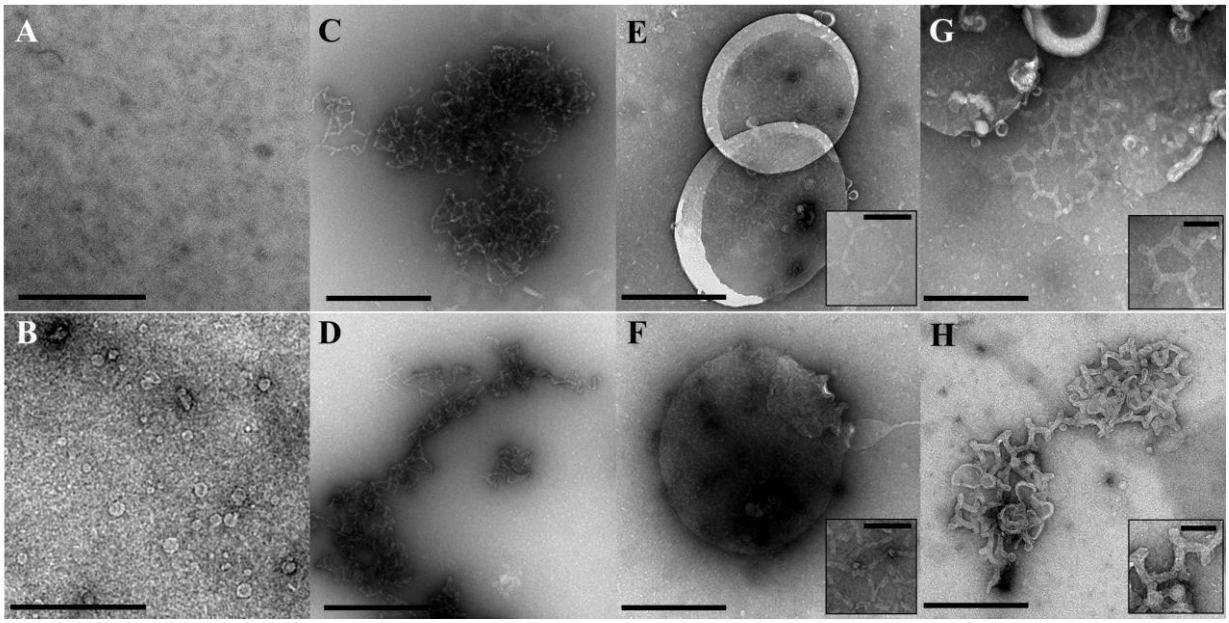

Figure S11: TEM micrographs of origami triskelia interacting with lipid monolayers. All samples were prepared as described in Fig $10. In each case, all steps of the protocol described in Fig S10 (steps A to H), or corresponding controls, were performed to allow for a direct comparison between the samples. Step A: 1 µL lipid in hexane added with a concentration between 0 mg/mL and 0.1 mg/mL. Step E: 5 µL of dimers of cholesterol-functionalized triskelia in 1×TE buffer +14 mM $MgCl_2$ added to give a final concentration of either 0 nM or 1 nM. Scale bars 500 nm (in insets 100 nm).

Control samples: (**A**) pure hexane and no triskelia: only the usual background corresponding to an empty grid is observed. (**B**) lipid in hexane (step A: 0.025mg/mL DOPC) and no triskelia produced a grid with a lighter background with small circles that we interpret as lipid aggregates on a lipid monolayer. The difference in the background between (A) and (B) is attributed to the presence of lipids on the grid.

Samples without lipid (step A: pure hexane): (**C**) flat and (**D**) curved triskelion dimers polymerized in the absence of lipid. These two grids produced triskelion aggregates similar to those observed during standard EM staining. Polymerized flat triskelia appear as dark and compact aggregates. Polymerized curved triskelia create more elongated aggregates.

Samples with optimal lipid concentration (step A: 0.025mg/mL DOPC): (**E**) flat and (**F**) curved dimers polymerized after the formation of a lipid layer on the EM grid. Large circular structures covered with polymerized triskelia are observed. Flat triskelia (**E**) produce a partially ordered array with hexagonal and pentagonal cells (see magnified inset). The micrograph of polymerized curved triskelia (**F**) shows a darker circular structure with a less-ordered and denser polymerization of the triskelia (see magnified inset).

Samples with excess lipid (step A: 0.1 mg/mL DOPC): (**G**) flat and (**H**) curved dimers polymerized after the formation of a lipid layer on the EM grid. Triskelia in both (**G**) and (**H**) appear larger than in (**E**) or (**F**), and the junctions between arms are not resolved (see magnified insets). We infer that the triskelia in (**G**), (**H**) are covered by an additional lipid layer. We hypothesize that excess lipids attach to the sides of the well and are not removed by washing during step D. After addition of the triskelia in step E, excess lipid detaching from the sides is then able to cover the triskelia attached to the lipid-covered grid.

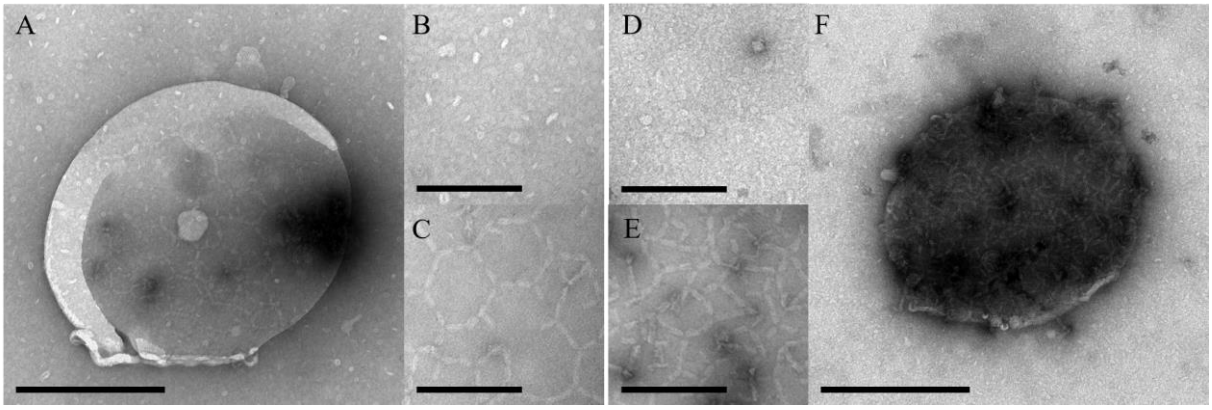

Figure S12: Flat and curved triskelia on lipid-covered EM grids. All images are electron micrographs of polymerized origami triskelia interacting with lipid monolayers, prepared as described in Materials and Methods and Fig S10. (**A**) and (**F**) show circular structures characteristic of flat and curved triskelia, respectively, interacting with the lipid monolayer. (**B**) and (**D**) show higher-magnification views of the surface of the grid (background) for flat (**B**) and curved (**D**) triskelia-containing samples. The irregularities appearing as small circles on the background are indicative of a lipid layer covering the grid (cf. Fig S11B). (**C**) and (**E**) show higher-magnification views of the triskelia-covered structures (flat and curved respectively). Flat triskelia are associated with the formation of light-colored circular shapes (**A**), with crescent boundaries consistent with collapsed blebs, covered with polymerized triskelia forming large and open meshwork (**C**). Curved triskelia are associated with the formation of heavily stained circular shapes (**F**) covered with compact meshwork (**E**). Scale bars A and F: 500 nm; scale bars B-E: 200 nm.

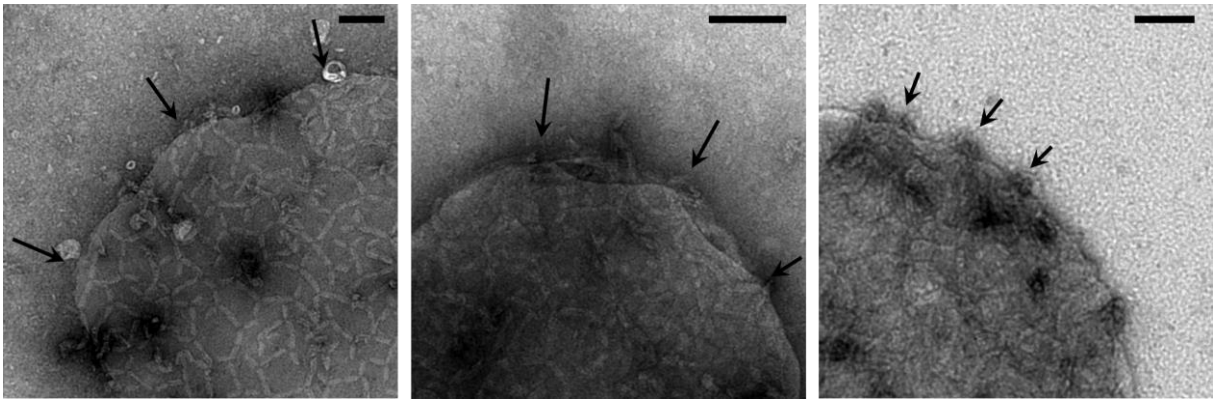

Figure S13: High-magnification electron micrographs showing nanoscale deformation of the lipid membrane by polymerized curved triskelia. Samples were prepared using the lipid monolayer assay described in the material and method, and Fig S10. The polymerized triskelia, which are easily distinguishable at this scale, form a partly-ordered meshwork on the lipid layer. Arrows indicate undulations of the edges of the large circular structures (only parts of which are shown here) which coincide with the curved shape of the triskelion, suggesting that the membrane and triskelia are in close contact and influence each other's geometries. Side views of the curved triskelia are visible indicating that, at the edge of the structure, the membrane is approximately perpendicular to the grid, consistent with a budding of the lipid membrane induced by the triskelia. Scale bars 100 nm.

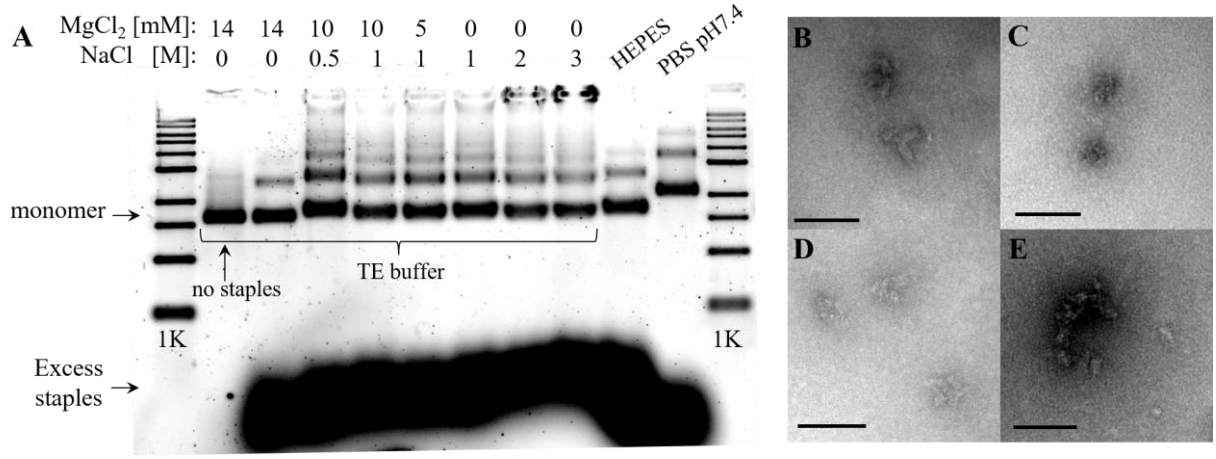

Figure S14: **Optimization of buffer conditions for experiments with triskelia interacting with GUVs**. The triskelion requires millimolar concentrations of a divalent cation such as Mg^{2+} or a much higher concentrations of monovalent cations to stabilize the multiple cross-overs within the DNA origami. In experiments with GUVs, magnesium ions have undesirable effects: they can mediate the binding of DNA origamis to lipid membranes even in the absence of cholesterol anchors and divalent cations are known to cause budding and tubulation in vesicles,[1] as well as cause them to adhere to one another.[2] High concentrations of monovalent cations create large osmotic pressures, and Na^+ is known to induce tubulation.[3] We investigated the effects of varying both Mg^{2+} and Na^+ concentration on origami.

(**A**) Electrophoretic analysis of flat triskelion monomers folded in different salt concentrations and buffers. The samples are in 1× TE with $MgCl_2$ and NaCl concentrations indicated, or in HEPES (20mM HEPES, 10 mM $MgCl_2$, 100 mM NaCl) or PBS buffer (pH 7.4, 140 mM NaCl, 3 mM KCl, 2 mM KH_2PO_4, 10 mM Na_2HPO_4), as indicated above the wells of the agarose gel. The presence of NaCl increases the concentration of dimers and multimers, which are observed as slower bands above the well-folded monomers. Above 1 M NaCl, aggregates of the DNA origami accumulate in the well. The strong reduction of mobility in PBS indicates misfolding.

(**B**-**E**) Electron micrographs of triskelia monomers extracted from slices cut from the gel. The slices were then thinly cut with a scalpel and pressed between two Parafilm®-protected microscope slides to extract the solution and recover the origami: (B) HEPES; (C) TE + 1 M NaCl; (D) TE +2M NaCl; and (E) PBS. Scales bars 100 nm. Triskelia folded in HEPES buffer showed no detectable misfoldings. High concentrations of NaCl (1M or above) induced the formation of tightly packed, amorphous DNA structures, independent of the concentration of $MgCl_2$.

In experiments with GUVs the concentration of Mg^{2+} was maintained at 10-14mM, large concentrations of monovalent cations were avoided, and the GUV suspension was diluted to reduce the probability of divalent cation-induced interaction between vesicles.

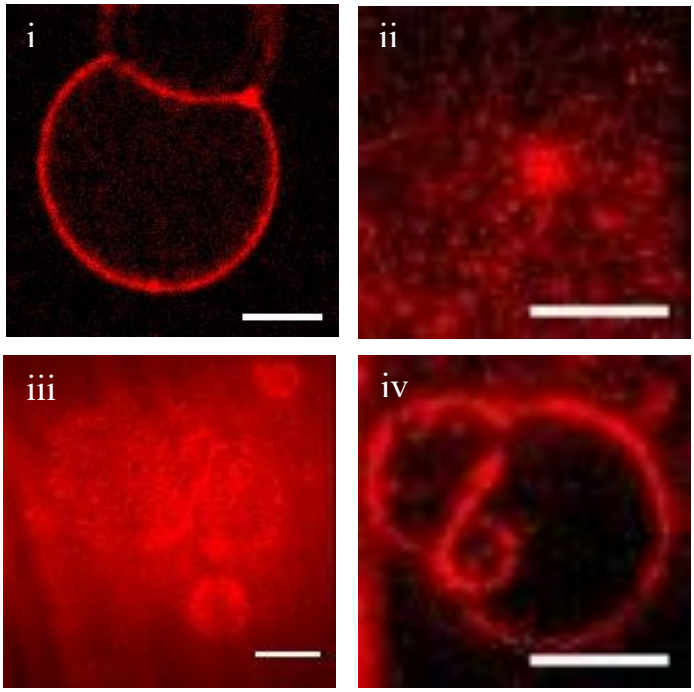

Figure S15: Additional micrographs of DNA triskelia on supported lipid bilayers and at GUV-SLB interfaces. These results correspond to those shown in Figure 4B but using DNA triskelia of different curvature.
TIRF micrographs of fluorescently labelled triskelia at GUV-SLB interfaces: (**i**) triskelia added to GUV before synapse formation are excluded from interface; (**ii**) triskelia added to GUV and polymerized before synapse formation inhibit interface formation; (**iii**) triskelia added to SLB before synapse formation are trapped at interface; (**iv**) triskelia added after synapse formation are excluded from interface. Triskelia used: flat (**i, iii**); curved (**ii, iv**). Scale bars 10 µm.

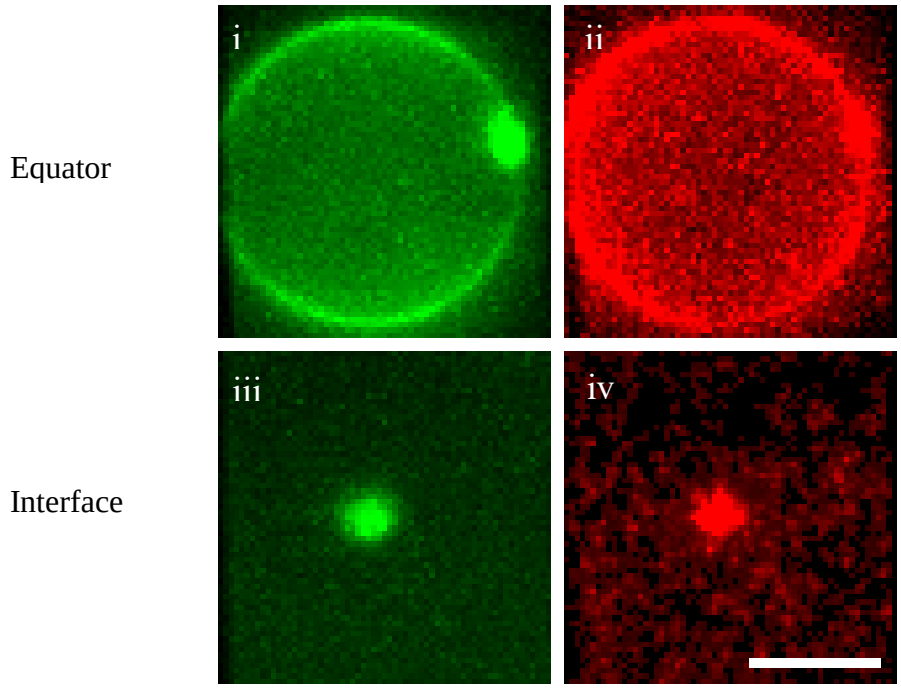

Figure S16: **Inhibition of GUV-SLB interface formation by polymerized triskelia.** Micrographs (epifluorescence (**i, ii**) and TIRF (**iii, iv**)) of equatorial and interfacial planes of the same GUV several minutes after it came in contact with a SLB. Both images were taken within a few seconds and show the same field of view with different depths of focus and imaging heights. The GUV included fluorescently labelled lipids (green) and was coated with fluorescently labelled, polymerized, curved triskelia (red). The contact area has not spread, consistent with inhibition of the formation of an extended SLB-GUV interface by the polymerized triskelia. Scale bars 10 µm

Fig. S17 CaDNAno routing
Triskelion

blue: DNA scaffold
black: main staples, common to flat and curved triskelia
red: staples bearing 6 bp sticky ends for polymerization (Arm 2 and Arm 3)
purple: dimerization strands (Arm 1)
green: strands bearing dye handle
yellow: strands bearing cholesterol handle

The last three lanes (HB 84, 85 and 87) are simplified representation of the bridges

arrangement of helices:

arm 1

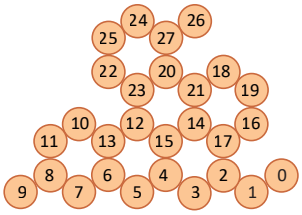

arm 2

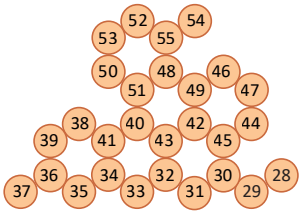

arm 3

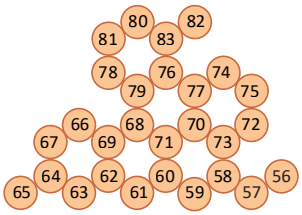

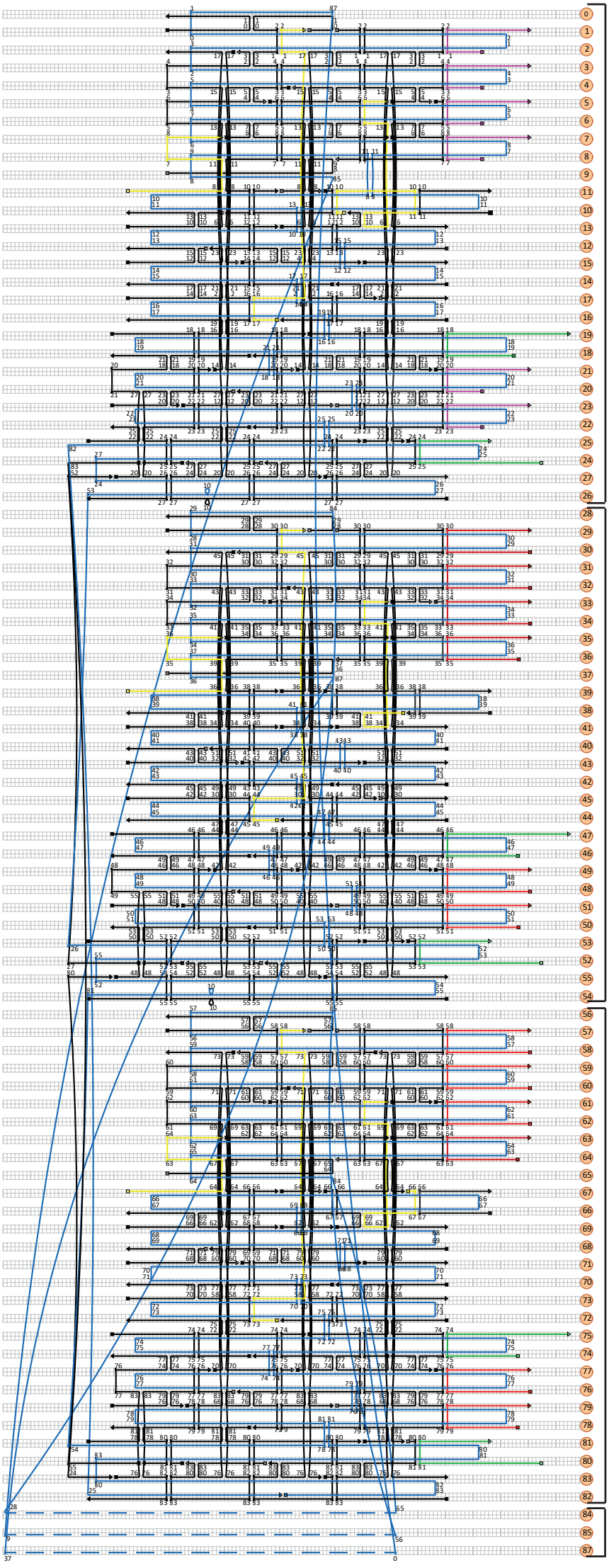

SI Movies

Supplementary Movie M1: Epifluorescence videos showing the diffusion of domains of polymerized DNA triskelia at the equatorial plane of a GUV. Scale bar 10 µm. Frame rate 50 Hz.

Supplementary Movie M2: Epifluorescence videos showing the diffusion of domains of polymerized DNA triskelia for an apical slice of the GUV. Scale bar 10 µm. Frame rate 50 Hz.

Supplementary Movie M3: Confocal z-stack of GUVs show homogeneously distributed lipids (green) and aggregated domains of polymerized DNA triskelia (red). Scale bar 10 µm.

Supplementary Movie M4: Confocal z-stack of GUVs show homogeneously distributed lipids (green) and unpolymerized DNA triskelia (red). Scale bar 10 µm.

DNA sequences

SEQUENCE TRISKELION

Sequences of black staples on CaDNAno file: common to all the triskelia

CORE and VERTEX STAPLES (black in caDNAno: see S17)

core_staple_45[95]33[108]	GAG CAA CAG TTT ACT AGA AAA AGC CTG TTT AAT AAA GCT AAA GTA TTC AGC TAT TC
core_staple_53[102]45[94]	GGA AGA GGT CAT TTT TGT TGA CCA GAA GCA AAA ACA GTA ATG CAG GTA A
core_staple_21[109]25[101]	AGG CGG GGT TGA GGG TTC GTA CTC AGG AGG TAG AA
core_staple_69[70] 71[90]	GTA ACG TAG ATG ATT ACC TTT TAC ATC GCA GAA ATA GCT CAT TTC GAT C
core_staple_21[74] 13[69]	CGG CAT ATC GGC CTT GCC ATG GAA TGG ATT AGG CCA AC
core_staple_67[70] 69[83]	GGC GCA TAA ACA TAT TTG AAT TAC CTT TCA AAA GAG CCG GAA
core_staple_71[91] 73[112]	GGT GCG GAT TTG CAT ATA ATC CTG ATT GTA AAA GTG GTT TTC CCA GTT TT
core_staple_16[112] 21[108]	TTT CGC AGT CTC TGA TTT GAT GAT ACA GGT GCC TTG TAA G
core_staple_68[112] 83[112]	TTT AGG CTG CGC AAC GGG AAA CTG CGC TCA CTA TTA AAG AAT TT
core_staple_19[77] 27[80]	AGA GTA GCG TCA TAT ATA AAC TAT TCT GGC GCC GCT ACA GGG TTA G
core_staple_63[98] 69[112]	TAC ATA ATA TTC ATC ATT CGC CAT TCT TT
core_staple_70[112] 74[98]	TTT TTA CGC CAG CTG AAA GTG TCA TAG CT
core_staple_81[102] 58[95]	GTG TGG CCC TGA GAG AGA GAG TCC ACT GCC CGA AGC ATG CGA AAG ACG CCA GTT G
core_staple_30[58] 46[63]	CGC GCC TGA TAT TAT ACA GAG GCA AAA GAA TTC TTT CC
core_staple_25[91] 10[87]	CAC CCT CTT AGT ACA TAA GTG CCA CCA CCA GAG GCC ACC CTC TCA G
core_staple_27[81] 24[66]	TAA GTG AGA ATA GAA AGG AAC AAC CGT CTT TAC TG
core_staple_52[45] 40[52]	CAT GCG GTT TAT CAG CTT TGA CAA CTC GCT GAT AGG
core_staple_15[60] 22[63]	GCT TGG TAA TAA ACA GGA GGC CCT TAT GGT TAC CAC

	CAG GAA GGG
core_staple_32[72] 44[70]	TAA CCA GTA ATA AGA GAA ATT GAG AAT TAC GAA TCA TCT TTG ACC
core_staple_33[109] 38[102]	CAA GAG AAC AGA CTT GCT GCT ATT TTG CAC CAC TTT AAC TG
core_staple_42[112] 46[98]	TTT CCA CAT TCA ACT TCA GAA AGA TAG CG
core_staple_43[91] 45[112]	CAG TTG AAA CGC GCG TAC CGA CAA AAG GCA ACG CTC AAC ACT ATC ATT TT
core_staple_83[81] 80[67]	GTT AAA CCG TCT ATC AGG GCG ATG GGG TTG AGG T
core_staple_79[84] 60[73]	ATG CAT TGG GCG CCA GTC GGT TGT ACC ACT CAT ATT AGG AAC TTA AAT CAA AG
core_staple_23[84] 4[73]	AAT GCG GCG CCA CCC TCG TGG CGA GAA ACA CCC GCT CTG AAA ATA CCT AAA TT
core_staple_35[56] 48[59]	AAG GCT TCC AAT AGA ACC GGA AGG CGC AGG CTT GCG CAT
core_staple_33[67] 38[56]	TGT ACC GCG CAT CCG GTA ACG CTA ACG AGC GCC AGA ACC AAA GCT
core_staple_57[84] 64[84]	GAA GTA TAC ATT ATT CAT CAA CGT AAA AGG AGA AAA CCT GAG TTT AAT GCT TAG AA
core_staple_41[70] 43[90]	TAC CCA AAA TCA TTA GAA ACC AAT CAA TTC AAC AAT TGA AAG AGT TCA T
core_staple_29[77] 33[66]	CAC CGG ATT CTG ACC TAA ATT TAA TGG TTA AAT AAA TAT TTA TTT CGA GGT CCT GAA GCA
core_staple_74[97] 70[84]	GTT TCC TAT GCC TGA AAC GAC GGC CAG TTT GGG TAG GGG ATG
core_staple_5[98] 15[112]	TTA TTC ATA AGT TTT TGA CAG GAG GTT TT
core_staple_4[72] 16[70]	CAT ATT ACG CAG TAT GTA ACC GAG CAA ATA ATA CTG TCC ATC ACG
core_staple_54[112] 53[90]	TTT CGC AAA TGG TCA ATA ACC TGT TTA GCA TTT AGT CGG ATG GGC AAA CT
core_staple_49[109] 53[101]	GAA GAC TAT TGA TTA AGT AAT TCG AGC TTC AGT CA
core_staple_77[109] 81[101]	CCT ATT GCG TCT GTC GTG GGA GAG GCG GTT TAC CA
core_staple_78[62] 77[52]	TAT GAC CAT AAA GCC CCA GCA GGC GAA AAA TAG CCG GGT GAG TGA T
core_staple_5[109] 7[97]	AGG GGG AAT TCG TCA GAT AGC CCC CTT ATT AGC GTT AAA AGT TTG
core_staple_79[46] 80[35]	GCA ACT TTT GCG GGA GAA AGA ATT TTG ATG G
core_staple_14[83] 19[76]	ATA TTC AAA CCT ATA GTT AAT GCC CCC TGA GTA AA
core_staple_39[81] 39[69]	GAG GAC GTT GGG AAA TCA ACG TAA GAG TAG T
core_staple_24[65] 21[73]	AGT GAC GGG GAA AGC CGG CGA ACA CCA TGT ACC GTA ACC CAG ACG CGC GTA CAT TT
core_staple_24[45] 12[52]	CTA CGG AGC CCC CGA TTT CGA AAG GTC ACG CTT GGC
core_staple_1[77] 5[66]	AAT AAG ACA AAG TCA GAG GGT AAT TGA GGA GTT AAA ATA ATA ACT CCT TAT GGT TTC CGA
core_staple_57[77] 61[66]	GGA TTT ATA TCT AAA ATA TCT TTA GGA GGA TAA TAA AGA AAC TGA TTA TTT GCG TAG TAA
core_staple_77[74] 69[69]	ACA AGA GGA AGA TTG TAA TTT TTG GCC ATC ATG AGC GA
core_staple_12[112] 27[112]	TTT CCG CCA CCA GAA CCG TCG ATT GCT CAT GGG ATT TTG CTT TT
core_staple_39[70] 41[83]	AAA TTG GTC TTA CCA TTC TAA GAA CGC GTC GTA GGG AAA AAT
core_staple_70[83] 75[76]	TGC TGC ACA ACA TAA TTG TTA TCC GCT CGT CTG GA
core_staple_80[45] 68[52]	CTG TAG CAA AAT TAA GCA CTG TAA TAG GAT AAT TCG

core_staple_11[81] 11[69]	TGA CGC CAC CCT TAG AAC CCT TCT AGT CTT T
core_staple_82[112] 81[90]	TTT CGT GGA CTC CAA CGT CAA AGG GCG AAT GGA ACA TTG CAG CTG GTT TT
core_staple_26[112] 25[90]	TTT AAA CAA CTT TCA ACA GTT TCA GCG GAA TGA ATT TAG GAA CGA ACC GC
core_staple_13[70] 15[90]	AGA GAC ATT ACC ATA GGG AGG GAA GGT AAA TAG AAC ATT TTG ACC CGC C
core_staple_23[45] 24[35]	GCG GAG CGG GCG CTA GGG CCT AAA GAA CGC CT
core_staple_42[83] 47[76]	ACG CCA ACC CTC AAA TCG TCA TAA ATA TAC ACT AA
core_staple_11[70] 23[83]	AAT GCG CAT ACC GAG TAA TCA GTA GCG AAG CAC CAG AAC CGC TCA ATC GCG CGC TT
core_staple_75[77] 83[80]	GCA AAC AAG CTT GCG TGT GAA CGA GCC GGC ATG CCT GAG TAA TCC A
core_staple_80[66] 77[73]	TTG CCT CAG AGC ATA AAG CTA AAG GAA GCG GTC CAC GCT GTG TTG TTG TGT AGT TCC
core_staple_81[91] 79[83]	TCT TTT CGC GTA TTT CCA GTC TGT TGG GAA GGG TTT AAC CAA ATT TTA A
core_staple_25[102] 17[94]	CCG GAT AGC AAG CCC AAT TCT GTA GTA CCA GAA ACA TGG ACG ATT TTA A
core_staple_40[112] 55[112]	TTT ACA ACA TTA TTA TCA AAA AAT AGT CAT TAG ATA CAT TTT TT
core_staple_46[97] 42[84]	TCC AAT AGC GAG AGC CAG ACG ACG ATA AAG GCA TAA TAC ATA
core_staple_61[98] 71[112]	GGA TTC GCA AAA TTG CCT CTT CGC TAT TT
core_staple_1[84] 8[84]	GCA AGA AAG AAG GAT AGC AAA CAC AAT CAA TAT TGC ACC AGT CAG AAT CCA TCG CC
core_staple_43[60] 50[63]	AAC GCT CCA TTT CAT GAG GAA GAT AAA GAC AAG GGA GTA GTT GCG
core_staple_5[67] 10[56]	TTG TAG CAA GCA GCA CCA CGA ACC ACC AGC AGG CTA TTG ACC TGA
core_staple_63[56] 76[59]	ATT TAA CAC ATC AAT TAA ATG AAA ATA AAA ATT TTT TCA
core_staple_15[91] 17[112]	GCC AGC AAT TTT GTC GTA GAA AAT ACA TCG AAC AAC AGA ATG GAA AGT TT
core_staple_67[81] 67[69]	ACC CCG CTT CTG AAC CCG TCG GAT GTA GAT G
core_staple_60[72] 72[70]	AAA CAG ATG ATG GCA ATC ATT TTG GAT TAA GGC CAA GAG AAT CGA
core_staple_41[84] 35[97]	CTA CGT TCA GTC AGA TGG TTT AAT TTC ACA GCT ACT TAG CGA
core_staple_52[65] 49[73]	AAT AGG TGA ATT TCT TAA ACA GAA CTT AGA GCT TAA TTC TGC GAA AGC AGC GTG AA
core_staple_22[62] 21[52]	AAG AAA GAG AGC TTT TCG TCA CCA GTA CAT CTA AAC GAG CAC GGG A
core_staple_14[112] 18[98]	TTT TGA GGC AGG TCA AAA GTA TAG TAA CA
core_staple_76[58] 80[46]	AAA CGA GAT AGC CCA CTA CGC CCA AAT CAA GTC AAA AGA TC
core_staple_49[74] 41[69]	TCC AAA ATC CGC GAC CTC GAA CTG ACA GAC CTA TTC AT
core_staple_18[97] 14[84]	GTG CCC GCA TGG CTA TTT ACC GTT CCA GAT CCT CAG GCC TTG
core_staple_20[58] 24[46]	TGA GTT TTG TTA AAG GAA TTG TTT TTT CAC GCG TAA CGA AA
core_staple_51[84] 32[73]	GCG GGC GCC AGA CCG GCT TGA TAC CGA TTA AAG GCA CGG TGT ACC AAC TTA GA
core_staple_33[98] 43[112]	CCT TAT CAA TGC AGG ATT TAG GAA TAT TT
core_staple_44[112] 49[108]	TTT AAC CCT CGT TTA GCT TTT GCA AAA GAT AGA CTG ACG A

core_staple_2[58] 18[63]	AAT TGA GTA GAC CGT TGT CAG TGA GGC CAC CGC GAT TA
core_staple_17[95] 5[108]	AGC AGT TAC CAC AAT GAA ATA GCA ATA GCT AAG ATA GCA CAT AAA CAC GGA ATT AA
core_staple_7[56] 20[59]	TCG ATA GGC CGG AAA CAT TCT TTT ACA TGC GCG TAG CTT
core_staple_53[91] 51[83]	CCA ACA GAA GCG AAG ATT GCA CAG GTA GAA AGA GAC AGA TGA CGC TTT T
core_staple_47[77] 55[80]	AAC ACA CCA AAA TAC TGC GGA ATG CTT TAG ATC GTC ACC CTC CGA G
core_staple_69[84] 63[97]	ACC AGG CTC CGG CAG TGC ATC TGC CAG TAT TTT CCG AAA CAG
core_staple_29[84] 36[84]	ATC ATA AAG GGC TTA TAT AAA CTG TTT AAA TCG GCA TTT TCA AGG CGT TAA TTT TA
core_staple_51[45] 52[35]	TCG GAA CCA TCG CCC ACG ATT GTA TTT TTA AA
core_staple_58[58] 74[63]	AGA TCA GAA ATA ATC GTG TCA TTG CCT GAG AAC CTG AT
core_staple_58[94] 61[108]	AGT ATA GAC TTT ACA AAC AAT TCG ATT AAT TTT TTG GAT ACC ATA TCC TG
core_staple_7[98] 13[112]	CCT TTA GAG AGC CAC CAC CCT CAG AGT TT
core_staple_72[112] 77[108]	TTT CAC GAC GTT GTA CAG GTC GAC TCT AGT CAT GGT AAA G
core_staple_71[60] 78[63]	TAA TAA GCA ACA ACC GTT CTA GAA GTA AAG ATA GAA CCA AAA CAT
core_staple_50[62] 49[52]	CCG ACA AGC TTT CGA TAA TGC TGT AGC TTA TAA CAA ACG AGG AGA C
core_staple_55[81] 52[66]	TAG TAT ATT TTC ATT TGG GGC GCG CCC AAT TGC TG
core_staple_48[58] 52[46]	CGG GTT GAT TAG CTG AAA AGT TCT ACT AAT ACA TTC CAC AA
core_staple_35[98] 41[112]	ACC TCC CAG CAA GCC GAA CTA ACG GAT TT
core_staple_61[109] 67[101]	ATT GGC GAA TAT CAA TAG TCG CTA TTA ATT ATT GA
core_staple_61[67] 66[56]	CAG GAA ACA AAA TTT CAG CGA TAG CTT AGA TCG TTG GTT CTC CGT
10[123]11[123] -not in contact	TTT GAA CCA GAG CCA CCA CAT AAT CAA AAT CAC CGT TT
38[123] 39[123] -not in contact	TTT TAT GCG ATT TTA AGA ATC ATT GTG AAT TAC CTT TT
66[123] 67[123] -not in contact	TTT GCC TCA GGA AGA TCG CGA CGA CGA CAG TAT CGT TT
triskelion_vertex 6T_21[53] 2[42]	GCT ATC CAG AAC TTG CCA CCC AAA AGT TTT TT
triskelion_vertex_6T_68[51] 58[59]	CGT AAA ATT CAG GTT TAA CTT TTT TTT TTT TAT TAT CAT CAT ATT CCC ACC
triskelion_vertex_6T_79[27] 82[21]	TTT TTT CCT TTA TTT GGA GAC ATT ATA AAT TTT TTG GGG TCG AGG TGC CG
triskelion_vertex_6T_12[51] 2[59]	AGA ACA GGA ACC AAA GAC ATT TTT TTT TTT TAA CTG GCA TGA TTA AGA CGG
triskelion_vertex_6T_46[62] 44[31]	ATT AAA CGG GTA AAA AAC GAA CAA GCG CGA AAC AAA GTA CTT TTT T
triskelion_vertex_6T_83[28] 74[27]	AAA TCC CGT TTT TTT TTT TTT CAA ATC ACC GCT ATT TTT TTT TTT
triskelion_vertex_6T_73[31] 70[31]	TTT TTT TAT GTA CCC CGG AAT TGT AAA CGT TTT TTT
triskelion_vertex_6T_9[42] 11[80]	TTT TTT ACA GAG GTG AGG CGG TCA GTA TTA ACA CCG CCT GCA AAT TAA AAG AAC
triskelion_vertex_6T_23[27] 26[21]	TTT TTT CTG GCA AGT GTG CTT TTA GTT AGT TGA AAA TCT CCA AAA AAA AG
triskelion_vertex_6T_74[62]	AAA TTA ATG CCG GAC TAT CAG AAA ACT AGC ATG TCA

72[31]	ATC ATT TTT T
triskelion_vertex_6T_18[62] 16[31]	AAG GGA TTT TAG ACT TTA TAA TAG CAA TAC TTC TTT GAT TTT TTT T
triskelion_vertex_6T_19[27] 23[44]	TTT TTT AAT CCT GAG AAG TGT TAG GAA CGT CAG AGC GTA TAA CGT A
triskelion_vertex_6T_41[31] 38[31]	TTT TTT CAA GAG TAA TCT CAG TGA ATA AGG TTT TTT
triskelion_vertex_6T_51[27] 54[21]	TTT TTT TAA CCG ATA CGG CTA CGA AGT TTG TAG TAG CAT TAA CAT CCA AT
triskelion_vertex_6T_65[41] 67[80]	TTT TTT GAG AAG AGT CAA TAG TGA ATT TAT CAA AAT CAT AGG TTC CTT GAC GTA
triskelion_vertex_6T_55[28] 46[27]	GTG TCT GAG TTT TTT TTT TTT AGG CTT TGA ATG CCA CTA TTT TTT
triskelion_vertex_6T_69[31] 66[31]	TTT TTT TAG CCA GCT TTC AAC GGC GGA TTG TTT TTT
triskelion_vertex_6T_77[53] 58[41]	ATT ATA TTT ATT GAT AAA GGA GCG GAT TTT TT
triskelion_vertex_6T_27[28] 18[27]	GCC CTC ACC TTT TTT TTT TTT TCG TTA GAA GTA CGC CAG TTT TTT
triskelion_vertex_6T_47[27] 51[44]	TTT TTT CGA AGG CAC CAA CCT AAT ACG TAG GAC TAA GTA GCA ATA T
triskelion_vertex_6T_17[31] 14[31]	TTT TTT AGT AAT AAC ATC ACA ATA TTA CCG TTT TTT
triskelion_vertex_6T_37[41] 39[80]	TTT TTT AGC CTA ATT TGC CAG TTA CAA AAT AAA CAG CCA TAT TTC CTG AAG CTT
triskelion_vertex_6T_40[51] 30[59]	CTG AAT CAT AAA ATA ATA TTT TTT TTT TTT TAT TTA GGC AGA GGC ATA CAA
triskelion_vertex_6T_49[53] 30[41]	TTT GTT ACT TTA TCA TCC AAC ATG TAT TTT TT
triskelion_vertex_6T_29[41] 28[41]	TTT TTT GTG ATA AAT AAG GCG TTT GAA ATA CCG ACC GTT TTT TT
triskelion_vertex_6T_15[31] 12[31]	TTT TTT CCA GCC ATT GCA TTC ACC AGT CAC TTT TTT
triskelion_vertex_6T_43[31] 40[31]	TTT TTT GCG CAG ACG GTC GCT GAC CTT CAT TTT TTT
triskelion_vertex_6T_75[27] 79[45]	TTT TTT GAG AGA TCT ACA AAG GGA GGG TAA TCA ATA AAA GGC CCA AC
triskelion_vertex_6T_1[41] 0[41]	TTT TTT ATA ACC CAC AAG AAT TCG CTA ATA TCA GAG AGT TTT TT
triskelion_vertex_6T_13[31] 10[31]	TTT TTT ACG ACC AGT AAT AGA ATA CGT GGC TTT TTT
triskelion_vertex_6T_57[41] 56[41]	TTT TTT ATT AGA GCC GTC AAT ACA CTA ACA ACT AAT AGT TTT TT
triskelion_vertex_6T_45[31] 42[31]	TTT TTT AAC GGA GAT TTG AGC CGG AAC GAG TTT TTT
triskelion_vertex_6T_71[31] 68[31]	TTT TTT TAA TAT TTT GTT CTG GCC TTC CTG TTT TTT
triskelion_vertex_6T_66[55] 71[59]	GGG AAC AAT CAA CAG AAA ACA AAT TTT TTT TTT TTG TCA GAT GAA TAT ACA GAT TTT CGC AT
triskelion_vertex_6T_10[55] 15[59]	AAG CGT AAA AAG GGA CGT CAC CAT TTT TTT TTT TTA AAG GGC GAC ATT CAA ACC AGC GAA AC
triskelion_vertex_6T_38[55] 43[59]	GCT CAT TTG ACA AGC AAG CAA ATT TTT TTT TTT TTC CCA TCC TAA TTT ACG ACA AGA AAG GG
extra_support_25[21] 22[27]	CAC TAA ATC GGA ACC GTT TTT T
extra_support_53[21] 50[27]	AAA AGG AGC CTT TAC ATT TTT T
extra_support_80[34] 55[27]	TGG TTC CGA AAT TTT TTT TTT TTT TGT ACG
extra_support_52[34] 27[27]	TAT GCA ACT AAA TTT TTT TTT TTT TTA GAC A

extra_support_81[21] 78[27]	ATA CAG GCA AGG CAA GTT TTT T
extra_support_24[34] 83[27]	GTA GCA TTC CAC TTT TTT TTT TTT TTC GGC A
78[127]79[127]	AAT CGG CCA ACG CGC GGC CAG CTG CAT TAA TG
50[127]51[127]	TTC AAA TAT CGC GTT TAG GAA GCC CGA AAG AC
22[127]23[127]	GGA ATA GGT GTA TCA CGA TAT AAG TAT AGC CC

STIFF BRIDGES

Common to both flat and curved bridges

Arm1_1_HB84	CGCCGGAGACAGAGAGAACCGCCAACGTGTTCCATCATAACTTAACACTTCCAGACTGGTCG
Arm1_2_HB84	CGCGGAAGTCCTACCGACCAACGCAGGACACATGAGGTCGAGTGCGGCAGTTGTTGTGCG
Arm1_3_HB84	CGCTTCTTCTGTACTATCTCTGTCGCACGCCGACTATAACTACTGTTGGTACAATGGCCG
Arm2_1_HB85	CGGTTCCTAGACCTAAGTAGAGATCCGAGAGTCTCAGGTGCCTCTATGACCGAGTCCTACCG
Arm2_2_HB85	CGCTCGGAGCGCAATGCAACTCCGGACCAACTGTGGATCCTGTCGTCGGACCGGACTGCG
Arm2_3_HB85	CGTGCATTCTCGCCATGTTCCGTCAGTACAAGTTGAAGAGTCGGTCACGTTAGAACAACG
Arm3_1_HB87	CGCCTCACTAACATGTAAGTGTAATTGAATGTGAGATTCAGCTCGAGAGACTAACACACAGC
Arm3_2_HB87	GCGCTGTCGTGCCGCACGTGTAAGTAAGGTTAGCGTACTGACAGGTCGAACCGGCGCTGC
Arm3_3_HB87	GCGGTCCAGTGACCGCCATTCGGACCGCTCTCACACACACGAATAACGAAGTCAAGGTGC
Arm1_2*_HB84	CAACACTAGGTTGGGTTATATAACTATATGTGCGAGAAAACTTTTTCAAAACACGT
Arm1_3*_HB84	TGGCGGGACTTCCGCGCGGCCCCTGCGTTGGTCGGTAGTTCTCTCTGTCT
Arm1_4*_HB84	TTTAACCTCCGGCTTAGTTATAGCCGCACTCGACCTCATGTGTATTGTAC
Arm2_2*_HB85	GTGACCGAATCTAAAGCATCACCTTGCTGAATGGTCAGTTGGCAAATCACTCTCGG
Arm2_3*_HB85	ATCTCCGCTCCGAGCGCGTTGCTCCGGAGTTGCATTGTACTTAGGTCTAG
Arm2_4*_HB85	CAGCAGCAAATGAAAACTCTTCCGACGACAGGATCCACAGTTCTTCTAAC
Arm3_2*_HB87	CGTTATTGTTTAACGTGAAAAATCAAAATAGCAGGGAAGCGCATTAGACCATTCAA
Arm3_3*_HB87	TTACACACGACAGCGCGCACCTTACTTACACGTGCGGCTTACATGTTAGT
Arm3_4*_HB87	AAGAAACGATTTTTTCGTGTGTCGACCTGTCAGTACGCTAACCTTGACTT

Strands specific to flat bridges (92 bp long)

Arm1_1*fl_HB84	CCGGCGCGACCAGTTAAGTTATGATGGCAAATATATTTTAGTTAATTTTTAAGTGTCTGGTTT

Arm1_5*fl_HB 84	GAGACTACGAGATAGGAAGAAGCGCGCACAACAACTGTCGGCGT GCGACACTTTTT
Arm2_1*fl_HB 85	GAACCGCGGTAGGAGAGGCACCTGAGAACAGTTGAAAGGAATTG AGGATTGTCATACTGCTTT
Arm2_5*fl_HB 85	GCCACGCTGAACATGGAATGCACGCGCAGTCCGGTCAACTTGTAC TGACGGAGAGC
Arm3_1*fl_HB 87	GAGGCGGCTGTGTCGAGCTGAATCTCAGGGAGAATTAACTGAACA CCCTTTCTCTGTTACTTT
Arm3_5*fl_HB 87	ATCCCAATAATGGCGCTGGACCGCGCAGCGCCGGTTGTGAGAGCG GTCCGCCAAAT

Strands specific to curved bridges (84 bp long)

Arm1_1*cu_HB 84	CCGGCGCGACCAGTTAAGTTATGATGGATATATTTTAGTTAATTT
Arm1_5*cu_HB 84	GAGACGAGATAGGAAGAAGCGCGCACAACAACTGTCGGCGTGCG ACATACCTT
Arm2_1*cu_HB 85	GAACCGCGGTAGGAGAGGCACCTGAGAGTTGAAAGGAATTGAGG A
Arm2_5*cu_HB 85	GCCACGAACATGGAATGCACGCGCAGTCCGGTCAACTTGTACTGA CGGCTGAG
Arm3_1*cu_HB 87	GAGGCGGCTGTGTCGAGCTGAATCTCAAGAATTAACTGAACACCC
Arm3_5*cu_HB 87	ATCCCAATGGCGCTGGACCGCGCAGCGCCGGTTGTGAGAGCGGTC CGAAT

DIMERIZATION STRANDS 3T (6 bp and 3T spacer arm 1-1)

2[121]1 [133] 1<->1, 6bp TTT	AAA AGT AAG CTC TTA CCG AAG CCC TTT TTT CGG CA
4[121]3 [133] 1<->1, 6bp TTT	GCA AAG ACA CGG TGG CAA CAT ATA AAT TTC CGA CT
6[121]5[133] 1<->1, 6bp TTT	TGA GCC ATT TTG AAT TAT CAC CGT CAT TTA GAA AC
8[121] 7[133] 1<->1, 6bp TTT	TTT TCG GTC ACT GTA GCG CGT TTT CAT TTT TTA AG
20[121]21[133] 1<->1, 6bp TTT	TTA GGA TTA GCT GAG ACT CCT CAA GAT TTG GAA TA
22[121]23[133] 1<->1, 6bp TTT	GGT GTA TCA CGA TAT AAG TAT AGC CCT TTG AAG GA

POLYMERISATION STAPLES (6 bp sticky ends arm 2-3)

30[133]29[133] 2<->3, 6bp	AGT CTG AC AAA TTC TTA CCA GTG TAT CAT ATG CGT TAT CAG TCA
32[133]31[133] 2<->3, 6bp	GCA CTG GA CAA TAA ACA ACA TGA TTC TGT CCA GAC GAC TAA CCG
34[133]33[133] 2<->3, 6bp	CGT GAT AA GTA CCG CAC TCA TCG AAC GGG TAT TAA ACC ATG CTC
36[129] 35[129] 2<->3, 6bp	TTT TTA AAT CAA GAT TAG TGG GAG GTT TTG AAG CCT AGC CA
48[133]49[133] 2<->3, 6bp	GGA CGT AT CAG GTC TTT ACC CTT GAC CAT AAA TCA AAA TCG TCC
50[133]51[133] 2<->3, 6bp	TTT TTC AAA TAT CGC GTT TAG GAA GCC CGA AAG ACC

	GCA TG
58[133]57[133] 3<->2, 6bp	CAG ACT CT TTG CCC GAA CGT TAC AAC TCG TAT TAA ATC TGA CTG
60[133]59[133] 3<->2, 6bp	CAG TGC GG AAG GGT TAG AAC CTT ATA CTT CTG AAT AAT CGG TTA
62[133]61[133] 3<->2, 6bp	ATC ACG TA CAA AAT CGC GCA GAG CTT TGA ATA CCA AGT GAG CAT
64[129] 63[129] 3<->2, 6bp	TTT CTT GCT TCT GTA AAT CTA TGT GAG TGA ATA AC TGG CTA
76[133]77[133] 3<->2, 6bp	ACG TCC GA GCT AAC TCA CAT TAG GGG TGC CTA ATG AGT GGA CGA
78[133]79[133] 3<->2, 6bp	TTT AAT CGG CCA ACG CGC GGC CAG CTG CAT TAA TG CAT GCG

DYE HANDLES

80[118]81[120] 5'-handle	TGC GAT ATT GCA TTA ATG CCC TTC ACC GCC AGA CGG GCA ACA GCT G
52[118]53[120] 5'-handle	TGC GAT ATT GCA TTA ATG CTC CTT TTG ATA TTA GAG AGT ACC TTT A
24[118]25[120] 5'-handle	TGC GAT ATT GCA TTA ACC CTC ATT TTC AGG CCA CCC TCA GAG CCA C
46[127]47[125] 3'-handle	GTA ATA GTA AAA TGT TAG TTT TGC CAG AGG TGC GAT ATT GCA TTA A
74[127]75[125] 3'-handle	GAG CTC GAA TTC GTA AAG GAT CCC CGG GTA TGC GAT ATT GCA TTA A
18[127]19[125] 3'-handle	GTT TTA ACG GGG TCA GAG TGT ACT GGT AAT TGC GAT ATT GCA TTA A

CHOLESTEROL HANDLES

lipid handle arm1_HB 1	CAA ATT AAA GAA CTC AAA CAA GAA ACG CGC CCA ATC ATT CTC CTA TTA CTA CC
lipid handle arm1_HB 5	AGC TAG CCC TAA TGC CAT CTT TTC CGG AAC CGC CTC CCA GAG CCA GCA AAA TAC GGA AAC ATT CTC CTA TTA CTA CC
lipid handle arm1_HB 7	TTT TTT ACA GAC AAT ATT TTT GAA TGA AGA TAA ATT TTT TTT TTT TAT GAA ACC ACA TTC TCC TAT TAC TAC C
lipid handle arm 2_HB 29	CCC AGC GAA ATT GTG TCG AGG AAT CGC CGA ATA AAC ATT CTC CTA TTA CTA CC
lipid handle arm 2_HB 33	GCT CAT TAT ACA ATA AAA CGT TTT TTG TCT TTC ATT CTC CTA TTA CTA CC
lipid handle arm 2_HB 35	TTT TTT CTT GCC CTG ACG AGA AAC ATC TTT CCA GTT TTT TTT TTT TCA GAT ATA GCA TTC TCC TAT TAC TAC C
lipid handle arm 3_HB 57	TGA ACG GAG CCC CAA AAA CGC CGG AAC ACA TTT GAC ATT CTC CTA TTA CTA CC
lipid handle arm 3_HB 61	GGG ACT CCA GCC AGC TTA AAG CGC TTC AAT TCA ATA ACC ATT CTC CTA TTA CTA CC
lipid handle arm 3_HB 63	TTT TTT ACC GTA ATG GGA TAG GTC ATA AGA CGC TTT TTT TTT TTT TAT TAA TTA CCA TTC TCC TAT TAC TAC C

Alexa647-DNA conjugate: /Alexa647/ TTA ATG CAA TAT CGC A
Cholesterol-DNA conjugate: GGT AGT AAT AGG AGA ATG /3CholTEG/

References SI:

1. Suzuki, Y.; Endo, M.; Sugiyama, H. Lipid-Bilayer-Assisted Two-Dimensional Self-Assembly of DNA Origami Nanostructures. *Nat. Commun.* **2015**, 6, 8052.
2. Komorowski, K.; Salditt, A.; Xu, Y.; Halenur Yavuz; Brennich, M.; Jahn, R.; Salditt, T. Vesicle Adhesion and Fusion Studied by Small-Angle X-Ray Scattering. *Biophys. J.* **2018**, 114, 1908-1920.
3. Schenk, N. A.; Dahl, P. J.; Hanna, M. G.; Audhy, A.; Tall, G.G.; Jefferson, D.; Anantharama, A. A Simple Supported Tubulated Bilayer System for Evaluating Protein-Mediated Membrane Remodeling. *Chem. Phys. Lipids* **2018**, 215, 18–28.